Spin-state transition in antiferromagnetic Ni$_{0.4}$Mn$_{0.6}$ films in Ni/NiMn/Ni trilayers on Cu(001)

T. Hagelschuer,[*] Y. A. Shokr, and W. Kuch[†]

Institut für Experimentalphysik, Freie Universität Berlin, Arnimallee 14, 14195 Berlin, Germany
(Received 4 September 2015; revised manuscript received 5 January 2016; published 26 February 2016)

The influence of the antiferromagnetic (AFM) spin structure of epitaxial Ni$_{0.4}$Mn$_{0.6}$ films on the magnetic properties of adjacent out-of-plane-magnetized ferromagnetic (FM) Ni layers in Ni/Ni$_{0.4}$Mn$_{0.6}$/Ni trilayers on Cu(001) is investigated by magneto-optical Kerr-effect experiments. An AFM interlayer coupling between the two FM layers, which emerges below the AFM ordering temperature for an odd number of atomic layers of the antiferromagnet, suddenly disappears at a lower, AFM-thickness-dependent transition temperature. For even numbers of atomic layers of the antiferromagnet, a maximum of the coercivity is observed at a corresponding temperature. This result is interpreted as a transition of the AFM spin structure of the Ni$_{0.4}$Mn$_{0.6}$ layer that strongly affects the interlayer exchange coupling of the two FM layers by direct exchange through the AFM layer.

I. INTRODUCTION

Antiferromagnets are a fascinating class of materials, not only because of their interesting physical properties, but also because of their high potential for applications. Thin films of antiferromagnetic (AFM) materials are already widely used in magnetoresistive thin-film devices as a means to control the magnetization of adjacent ferromagnetic (FM) layers [1]. The use of AFM materials has also been proposed as a possible recipe to stabilize the magnetization of nanometer-sized particles at room temperature [2]. Recently, magnetoresistive effects in AFM materials themselves have become the focus of interest [3]. Antiferromagnets may thus play a principal role as active components in future spin-electronic devices. It has been demonstrated that if the AFM spin structure can be controlled, it may be used to store information [4,5], analogously to data storage in FM media.

Due to geometric frustration of AFM nearest-neighbor interactions, unlike ferromagnets, antiferromagnets can exhibit a rich variety of different spin structures. An example is the fcc lattice, in which nearest-neighbor AFM exchange interactions are frustrated. This may lead to noncollinear spin structures [6–9]. Although the knowledge of the spin structure is a basic prerequisite for the use of AFM materials in devices, experimentally its investigation is not an easy task. Neutron scattering can detect the AFM spin structure, but requires large samples and is thus not applicable to thin films and nanostructures. Spin-polarized scanning tunneling microscopy, which has contributed considerably to our understanding of complex AFM spin structures at surfaces [4,10–13], does not sense the spin structure in the interior of thin films or in buried layers. Thus, one has to resort to indirect methods. The interlayer coupling between two FM layers across an AFM spacer layer by direct exchange interaction between nearest-neighbor atoms within the AFM spacer and at the interfaces, for example, contains information about the spin structure of the antiferromagnet

[14]. The AFM spin structure directly affects the exchange coupling at the interface between the FM and the AFM material [15]. For a given interface structure and morphology, changes in the interlayer coupling can thus be attributed to changes in the magnetic state of the AFM spacer layer as long as the magnetic properties of the FM layers stay the same.

In this paper, we report on a temperature-induced change of the spin state of a Ni$_{0.4}$Mn$_{0.6}$ layer sandwiched between perpendicularly magnetized FM Ni layers. The coupling between the Ni layers is deduced from minor-loop measurements by the magneto-optical Kerr effect (MOKE). Below the ordering temperature of the AFM layer, a strong coupling between the two FM layers is evident. The sign of this coupling oscillates with a period of two atomic monolayers (ML) as a function of the Ni$_{0.4}$Mn$_{0.6}$ spacer layer thickness—a clear indication for coupling by direct exchange. At a certain lower temperature, which depends on the thickness of the AFM layer, this interlayer coupling suddenly disappears. This is interpreted as a temperature-driven spin-reorientation transition of the AFM spin structure, which affects the magnetic coupling at the AFM/FM interface.

Ni$_x$Mn$_{1-x}$ films around the equiatomic composition are known to grow in a tetragonal structure on Cu(001), where the bulk *a* and *c* axes are lying in the film plane and are strained to the Cu lattice constant, such that Ni and Mn planes alternate in the in-plane [100] direction [13,16]. Ni$_x$Mn$_{1-x}$ on Co/Cu(001) exhibits antiferromagnetism at Ni concentrations $x \leqslant 0.6$ [16]. Spin-polarized scanning tunneling microscopy revealed a noncollinear spin structure within the film plane in 12 ML Ni$_{0.5}$Mn$_{0.5}$/Cu(001) at room temperature [13].

II. EXPERIMENT

The experiments were performed in an ultrahigh vacuum chamber operating at a base pressure of 5×10^{-11} mbar. The single-crystalline Cu(001) substrate was prepared by cycles of sputtering with Ar$^+$ ions of 1 keV energy and subsequent annealing to 820 K for 30 minutes. The surface quality was verified by low-energy electron diffraction, which showed a sharp $p(1 \times 1)$ pattern. The different materials were thermally evaporated by electron bombardment of high-purity (Ni: 99.99%, Mn: 99.98%) rods at pressures of 5×10^{-10} mbar

---

[*]Present address: Deutsches Zentrum für Luft- und Raumfahrt, Institut für Optische Sensorsysteme, Rutherfordstraße 2, 12489 Berlin, Germany.

[†]Corresponding author: kuch@physik.fu-berlin.de

for Ni and 9×10^{-10} mbar for Mn onto the sample held at room temperature. The deposition of the AFM $Ni_{0.4}Mn_{0.6}$ alloy was realized by coevaporation of the constituents. To calibrate the film thickness, *in situ* medium-energy electron diffraction (MEED) and Auger electron spectroscopy (AES) were performed. Ni shows characteristic MEED oscillations up to about 5 ML, as shown in Ref. [17]. Under the condition that the concentration of Ni is $x \gtrsim 0.4\%$, growth of Ni_xMn_{1-x} can also be controlled by MEED [16]. Alloys of varying layer thickness with composition around $Ni_{0.4}Mn_{0.6}$ were grown on top of Ni/Cu(001). $Ni_{0.4}Mn_{0.6}$ grows on Cu(001) in a tetragonally expanded fct structure with the c axis parallel to the surface [16]. Since the lateral lattice constant of ultrathin Ni/Cu(001) is identical to that of the pure substrate, it is assumed that the morphology of $Ni_{0.4}Mn_{0.6}$ remains unchanged by the additional Ni underlayer. The Ni top layer was deposited using the same parameters as for the bottom layer. The thicknesses of both the top and bottom Ni layers were chosen as 15.0 ML, which is in the range of perpendicular magnetic anisotropy [18–20]. The AFM $Ni_{0.4}Mn_{0.6}$ layer was prepared with thicknesses of 6.0, 9.0, 11.0, 12.0, and 15.0 ML. To ensure that thickness and composition of the multilayer system are correct, AES measurements as discussed in Ref. [21] were performed after evaporation of each layer. This yields a statistical error of ± 0.1 ML for the thickness and ± 0.02 for the Ni and Mn concentrations, while the respective systematic errors could be about three times larger.

The optical polar MOKE setup contains a diode laser emitting monochromatic linearly polarized light of 1 mW power at a wavelength of 670 nm. The laser beam enters and exits the UHV chamber through special windows made of quartz glass, which reduced the Faraday effect to a negligible level. The magnetic field was generated by two electromagnets placed on opposite sides of the sample with the coils at air and the cores reaching into the vacuum. MOKE was measured using a photoelastic modulator operated at 50 kHz and recording the $2f$ signal of a lock-in amplifier, which is proportional to the Kerr rotation [22]. All Kerr intensities are presented on the same absolute scale.

Before deposition of the NiMn AFM layer, the bottom Ni layer was magnetized in a field of -150 mT at room temperature along its easy axis, normal to the surface plane. The NiMn/Ni bilayers were cooled to 40 K in a field of -150 mT and subsequently measured by *in situ* polar MOKE, increasing the temperature stepwise up to 340 K. Before deposition of the top Ni layer, the sample was again magnetized in a -150 mT magnetic field. Major and minor loops of the trilayer sample were then measured while increasing the temperature up to 480 K after cooling the sample to 40 K in remanence.

III. RESULTS AND DISCUSSION

Figure 1(a) presents magnetization curves of a 15 ML Ni/15 ML $Ni_{0.42}Mn_{0.58}$/15 ML Ni/Cu(001) trilayer for some temperatures. From 40 up to 320 K, the loops do not change much, except for some small exchange bias that is observed below 210 K [23]. Starting at 325 K, the loops split and two jumps of the magnetization are observed in each branch. At the same time, the field necessary to saturate the sample increases.
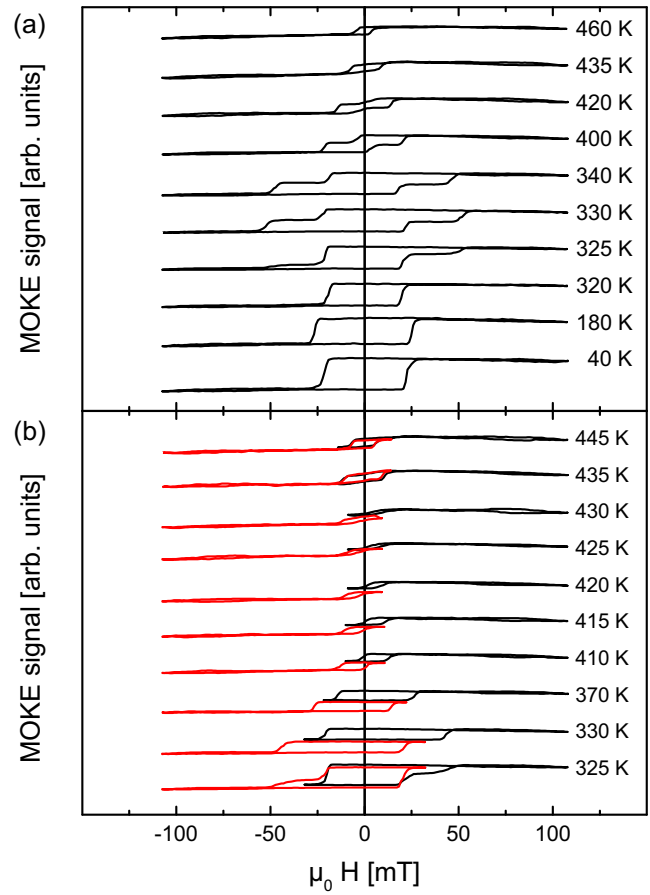
FIG. 1. (a) Major magnetization loops of 15 ML Ni/15 ML $Ni_{0.42}Mn_{0.58}$/15 ML Ni/Cu(001) in the range of 40–460 K and (b) selected minor loops of the same system in the range of 325–445 K. Above a transition temperature $T_T \approx 325$ K, the loops indicate AFM coupling between the two FM layers. The coupling disappears above the antiferromagnetic ordering temperature of ≈ 435 K.

The reduced remanence at 420 K indicates that this is due to an antiparallel interlayer coupling between the two FM Ni layers. To further prove this and to rule out that the loops are simply caused by two uncoupled layers with different coercivities, minor loops at temperatures $\geqslant 325$ K were measured and are presented in Fig. 1(b). When coming from saturation, the field was reversed between the two jumps of the magnetization, indicated by the end of the lines in Fig. 1(b). Black and red curves are for positive and negative saturation of the sample, respectively. A shift of the center of the minor loops away from zero field is evident, from which the strength of the antiparallel interlayer coupling J can be calculated as $J = M_S t \mu_0 H_{shift}$, where M_S denotes the magnetization, t the thickness of the reversing FM layer, and H_{shift} the shift field of the minor loop. The coercivity of the minor loops just above the transition temperature $T_T = 325$ K is larger than that of the single-step loops just below that temperature. From the minor loops, it can also be excluded that below T_T, the second step in the loops is not just absent because the coercivity of one of the FM layers exceeds the maximum available magnetic field. A comparison shows that the MOKE intensities below and above $T_T = 325$ K are equal. This ensures that all of the observed
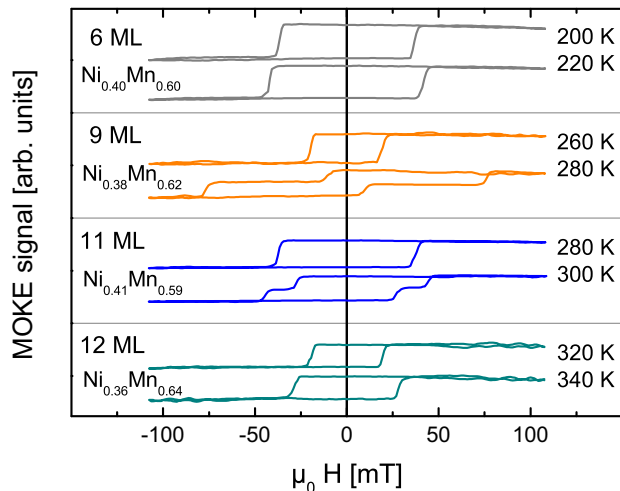
FIG. 2. Magnetization loops at temperatures below and above the transition temperature T_T for different AFM layer thicknesses. Antiparallel coupling is only observed if the number of atomic layers is odd. For layers containing an even number of atomic layers, only H_C is enhanced when increasing the temperature across T_T.

Kerr signal stems from both Ni layers and all of the curves in Fig. 1(a) are indeed major loops. The antiparallel coupling gradually decreases with increasing temperature and vanishes at about 435 K. At this temperature, the coercivity approaches that of the individual Ni layers [24], showing a distinct kink in its temperature dependence. We define this temperature as the antiferromagnetic ordering temperature T_{AF}.

The temperature-dependent transition to the AFM coupling depends on the AFM layer thickness, as shown in Fig. 2. It shows pairs of magnetization loops for the different NiMn layer thicknesses besides the data shown in Fig. 1, each for one temperature just below and one just above the transition temperature. Antiparallel coupling, as seen from the double-step loops at 9 and 11 ML NiMn thickness, only occurs if the AFM layer thickness is an odd number of monolayers. In the case of an even number of NiMn monolayers, such as 6 and 12 ML, the respective transition is characterized by only an increase in the coercivity for increasing temperature. This is more clearly visualized in Fig. 3(a), which shows the coercivity as a function of temperature for all of the investigated samples. In the case of antiparallel interlayer coupling, the coercivity of the individual layers was measured as half the field difference between the first step on one side and the second step on the other side of the major magnetization loop. A change in coercivity at the transition temperature is obvious for 9 and 15 ML NiMn, but also present at some other thicknesses. The reason for the more continuous change at T_T for 11 ML NiMn could be due to a slightly different thickness of the bottom Ni layer or of the NiMn layer within the accuracy of the thickness determination. The coercivity can depend quite sensitively on the exact layer filling at the interface [25].

Minor loops with a second step, such as the one at 325 K in Fig. 1(b), are observed only right at the transition temperature. They can be viewed as a superposition of the minor loops observed just above and below the transition temperature. This could be either due to a laterally inhomogeneous transition
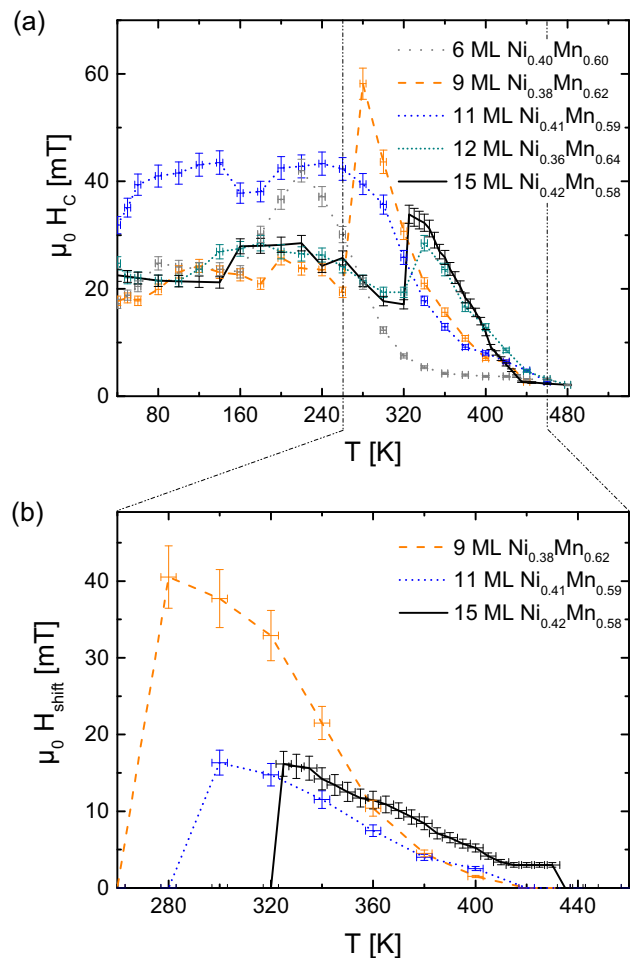
FIG. 3. (a) Coercivity H_C for all samples and (b) offset of the minor loops from zero field H_{shift} for samples with odd AFM layer thicknesses as a function of temperature. The phase transition is accompanied by an increase of H_C with increasing temperature, and the appearance of antiparallel coupling for odd-layer thicknesses of the AFM layer. H_{shift} is proportional to the coupling strength and is reduced for thicker AFM layers.

on the sample due to local thickness fluctuations or a small temperature gradient, or the consequence of a temporal superposition during the course of the measurement in the presence of a small temperature drift.

Figure 3(b) presents the shift field of the minor loops in the case of antiparallel coupling, which is proportional to the coupling strength. Just above the respective transition temperature, the coupling is strongest, reaching its maximum of $J_{max} = 1.8 \times 10^{-5}$ J/m^2 at a thickness of 9 ML NiMn. At higher temperatures, the coupling decreases gradually and reaches zero at the ordering temperature of the AFM layer.

The even/odd dependence of the interlayer coupling on the AFM layer thickness and its disappearance above the AFM ordering temperature strongly suggest direct exchange coupling through the AFM spin structure as the origin of the observed antiparallel interlayer coupling. Normally one would expect that this coupling should continue to increase for decreasing temperature. In the NiMn films, however, it suddenly disappears below a certain temperature T_T. The
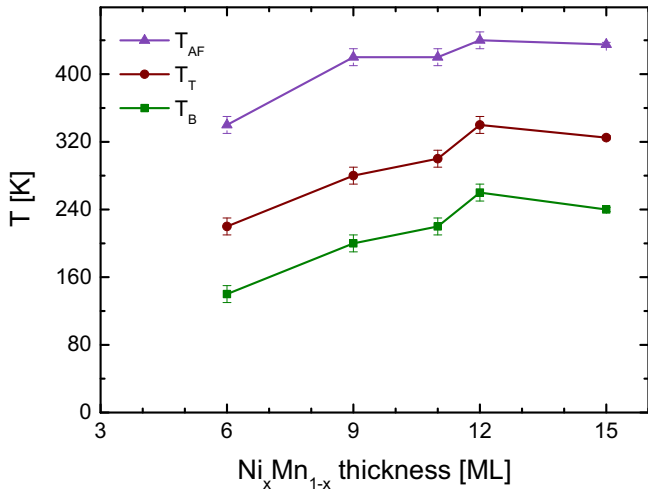
FIG. 4. Blocking temperature for exchange bias T_B, transition temperature of the spin-state transition T_T, and antiferromagnetic ordering temperature T_{AF} as a function of the $Ni_{0.4}Mn_{0.6}$ thickness. All characteristic temperatures increase in the same way. The exact compositions of the Ni_xMn_{1-x} layers are the same as listed in the legend of Fig. 3(a). Slight deviations from a smooth variation are possibly due to the slight variations in the composition of the AFM alloy.

interpretation of this behavior thus requires a different approach. We propose a transition within the AFM spin structure at T_T to explain our results. This may be a spin-reorientation transition from a complex noncollinear to a layerwise collinear AFM spin structure. Since the latter is expected to couple more strongly to an adjacent FM layer, it would lead to a more effective interlayer coupling by direct exchange. Also, a spin-reorientation transition between a predominantly in-plane and an out-of-plane AFM spin structure could alter the exchange coupling at the AFM-FM interface, leading to the observed change in interlayer coupling.

The transition temperature itself increases with increasing NiMn thickness, as shown in Fig. 4 by solid squares. Although less obvious than for the odd-monolayer thicknesses, the temperature of the singular sudden drop of the coercive field with decreasing temperature in the AFM layers with even-layer thickness within an otherwise continuous behavior of $H_C(T)$ [Fig. 3(a)] falls well into the temperature dependence of the disappearance of antiparallel coupling in the AFM layers with an odd number of monolayers. It is thus plausible that the same spin-state transition is also present in AFM layers with an even number of monolayers.

Figure 4 compares the transition temperature T_T to the blocking temperature of exchange bias T_B and the AFM ordering temperature T_{AF}. The latter is defined as the temperature below which the antiferromagnetic order of the AFM layer becomes evident in the trilayer by affecting the magnetization reversal of the FM layers, leading to a kink in the temperature dependence of the coercivity [16,21,24,26]. Note that this is not necessarily identical to the Néel temperature of the free antiferromagnetic layer. The appearance of antiferromagnetic order might be modified by the presence of the FM layers [24,27]. Furthermore, antiferromagnetic order

might be present at higher temperatures, without affecting the magnetization reversal of the FM layers [27,28]. The three temperatures show identical characteristics as a function of AFM layer thickness. The fact that T_T for 15 ML $Ni_{0.42}Mn_{0.58}$ is slightly reduced compared to 12 ML $Ni_{0.36}Mn_{0.64}$ can be explained by the different composition of both alloys. Since the concentration of Ni is higher in the former, T_T is shifted to lower temperatures, as is known for T_B and T_{AF} from earlier studies on AFM ordering temperatures [26].

A spin-reorientation transition between in plane and out of plane as a function of thickness has been reported for AFM NiO films in NiO/CoO bilayers [29]. It had been attributed to the competition between the intrinsic anisotropy and the interfacial exchange coupling, where the relative weight of the latter decreases with increasing layer thickness. A similar scenario could also be discussed for our case: The interaction with the out-of-plane-magnetized FM layers could lead to an out-of-plane AFM spin structure above a certain temperature, while below an in-plane or three-dimensional noncollinear spin structure might be stable. Alternatively, one could consider a competition between interface and bulk anisotropies of the NiMn layer. In both cases, however, one would expect that a thinner AFM layer would be more strongly influenced, such that a higher transition temperature would result for smaller thicknesses [29]. The result shown in Fig. 4 rather suggests that the spin-state transition at T_T is a further intrinsic characteristic property of the AFM layers, besides the blocking of exchange bias at T_B and the disappearance of AFM order at T_{AF}.

The disappearance of interlayer coupling below a certain temperature has also been observed in Fe/Cr(001) superlattices [30]. In this case, a nonoscillatory biquadratic coupling across the Cr layers disappears below their Néel temperature. This has been attributed to the pinning of spins at the interface in the antiferromagnetically ordered phase that mediates the biquadratic coupling above the Néel temperature [30]. In our case, a collinear oscillating interlayer coupling is present in a temperature range between two limiting temperatures. Following the explanation of the Fe/Cr case, one could try to interpret the lower of these two temperatures as the Néel temperature. However, it would then not be clear why a collinear interlayer coupling should disappear at temperatures below the Néel temperature, and how the upper temperature should be explained. Kinks in the coercivity as a function of temperature, such as the ones observed here at that upper temperature, have been observed in several systems before and are characteristic for the manifestation of antiferromagnetic order in AFM/FM bilayers or FM/AFM/FM trilayers [16,21,24,26]. We thus assign the upper temperature to the antiferromagnetic ordering temperature, while the lower one has to be interpreted as an additional transition in the antiferromagnetic spin structure.

Figure 5 shows the temperature dependence of the exchange bias field H_{EB} of all samples. Figure 5(a) presents H_{EB} of the NiMn/Ni bilayers before deposition of the top Ni layer, and Fig. 5(b) presents the exchange bias fields of the corresponding trilayers. The thickness dependence of the blocking temperature T_B in Fig. 4 has been extracted from these data. Comparison of H_{EB} of the bilayer and trilayer data shows that in all cases, the exchange bias at a fixed temperature as well as T_B are reduced after deposition of the

FIG. 5. Temperature dependence of the exchange bias field H_{EB} of (a) the $Ni_{0.4}Mn_{0.6}/Ni$ bilayers before deposition of the top FM Ni layer, and (b) the $Ni/Ni_{0.4}Mn_{0.6}/Ni$ trilayers.

existence of pinned moments or pinning centers, while at the same time the interlayer coupling by direct exchange is much weaker. This could be the consequence of a complex three-dimensional noncollinear spin structure [9,14,32,33]. A remaining small antiparallel interlayer coupling below T_T may be overcompensated by ferromagnetic coupling due to magnetostatic interactions between domain walls [34,35] during the magnetization reversal, such that no separate loops of the two FM layers can be observed for any of the samples below T_T.

Finally, it is also necessary to discuss why the antiparallel coupling above T_T occurs for odd- and not for even-layer thicknesses. For any AFM spin structure in which the orientation of magnetic moments changes layerwise and the coupling to an adjacent FM layer is identical at both interfaces, antiparallel coupling is expected to arise at even-layer thicknesses and parallel coupling at odd-layer thicknesses. Our results thus indicate that the effective AFM layer thickness for direct exchange coupling is reduced by 1 ML with respect to the real thickness. This difference between effective and real AFM thickness might be due to monoatomic steps at the interface always present even at layer-by-layer growth. In single-crystalline FeNi/FeMn/Co trilayers epitaxially grown on Cu(001), the phase of the oscillatory direct exchange coupling across the AFM FeMn layer changes up to 1 ML with the layer filling of the bottom Co FM layer, such that antiparallel coupling could be observed at an odd or an even number of FeMn atomic layers, depending on the exact thickness of the Co bottom layer [14].

IV. CONCLUSIONS

Ultrathin AFM $Ni_{0.4}Mn_{0.6}$ films sandwiched between out-of-plane-magnetized Ni layers on Cu(001) exhibit a transition in the spin structure at a temperature between the blocking temperature for exchange bias and the antiferromagnetic ordering temperature T_{AF}. If the thickness of the AFM layer is an odd number of monolayers, the spin structure present above this transition temperature leads to a significant antiparallel interlayer coupling. This is mediated by direct exchange coupling through the AFM spin structure, which disappears at T_{AF}. The effective thickness for direct exchange is thereby reduced by 1 ML with respect to an ideal model of layerwise AFM coupling, most likely because of monoatomic steps at the interfaces. Exploiting the transition of the spin structure could be a way of controlling the magnetic properties of a multilayered magnetic system by taking advantage of the sudden onset of interlayer coupling, the corresponding jump in coercivity, or the change in the AFM spin structure itself.

top FM layer. This indicates that pinned magnetic moments are distributed across the bulk of the AFM layer, where individual pinning centers contribute exchange bias only to one of the FM layers. This reduces the effective AFM layer thickness for exchange bias for each of the FM layers, which have to compete for the pinning centers, as has been discussed in Ref. [31].

What is remarkable is that exchange bias only occurs at temperatures below the transition in the AFM spin structure. Exchange bias and the strong direct exchange coupling hence are not present at the same time. Exchange bias generally needs two ingredients: magnetic interface coupling between FM and AFM layers, and pinned moments in the AFM layer that do not reverse, or at least not completely, upon magnetization reversal of the FM layer. Obviously, the AFM spin structure that is present in the NiMn films above the transition temperature lacks pinned moments, and all of the AFM spins reverse together with the FM layers. The observed exchange bias below the blocking temperature T_B proves the

[1] B. A. Gurney, M. Carey, C. Tsang, M. Williams, S. S. P. Parkin, R. E. Fontana, Jr., E. Grochowski, M. Pinarbasi, T. Lin, and D. Mauri, in *Ultrathin Mag-* *netic Structures IV: Applications of Nanomagnetism*, edited by B. Heinrich and J. A. C. Bland (Springer, Berlin, 2005), pp. 149–174.

[2] V. Skrumryev, S. Stoyanov, Y. Zhang, G. Hadjipanayis, D. Givord, and J. Nogués, Nature (London) **423**, 850 (2003).

[3] B. G. Park, J. Wunderlich, X. Mart, V. Holý, Y. Kurosaki, M. Yamada, H. Yamamoto, A. Nishide, J. Hayakawa, H. Takahashi, A. B. Shick, and T. Jungwirth, Nat. Mater. **10**, 347 (2011).

[4] S. Loth, S. Baumann, C. P. Lutz, D. M. Eigler, and A. J. Heinrich, Science **335**, 196 (2012).

[5] X. Marti, I. Fina, C. Frontera, Jian Liu, P. Wadley, Q. He, R. J. Paull, J. D. Clarkson, J. Kudrnovský, I. Turek, J. Kuneš, D. Yi, J.-H. Chu, C. T. Nelson, L. You, E. Arenholz, S. Salahuddin, J. Fontcuberta, T. Jungwirth, and R. Ramesh, Nat. Mater. **13**, 367 (2014).

[6] J. S. Kouvel and J. S. Kasper, J. Phys. Chem. Solids **24**, 529 (1963).

[7] H. Umebayashi and Y. Ishikawa, J. Phys. Soc. Jpn. **21**, 1281 (1966).

[8] K. Nakamura, T. Ito, A. J. Freeman, L. Zhong, and J. Fernandez-de-Castro, Phys. Rev. B **67**, 014405 (2003).

[9] W. Kuch, L. I. Chelaru, F. Offi, J. Wang, M. Kotsugi, and J. Kirschner, Phys. Rev. Lett. **92**, 017201 (2004).

[10] S. Heinze, M. Bode, A. Kubetzka, O. Pietzsch, X. Nie, S. Blügel, and R. Wiesendanger, Science **288**, 1805 (2000).

[11] M. Bode, M. Heide, K. von Bergmann, P. Ferriani, S. Heinze, G. Bihlmayer, A. Kubetzka, O. Pietzsch, S. Blügel, and R. Wiesendanger, Nature (London) **447**, 190 (2007).

[12] C. L. Gao, U. Schlickum, W. Wulfhekel, and J. Kirschner, Phys. Rev. Lett. **98**, 107203 (2007).

[13] C. L. Gao, A. Ernst, A. Winkelmann, J. Henk, W. Wulfhekel, P. Bruno, and J. Kirschner, Phys. Rev. Lett. **100**, 237203 (2008).

[14] W. Kuch, L. I. Chelaru, F. Offi, J. Wang, M. Kotsugi, and J. Kirschner, Nat. Mater. **5**, 128 (2006).

[15] K. Nakamura, A. J. Freeman, D.-S. Wang, L. Zhong, and J. Fernandez-de-Castro, Phys. Rev. B **65**, 012402 (2001).

[16] C. Tieg, W. Kuch, S. G. Wang, and J. Kirschner, Phys. Rev. B **74**, 094420 (2006).

[17] J. Lindner, P. Poulopoulos, R. Nünthel, E. Kosubek, H. Wende, and K. Baberschke, Surf. Sci. **523**, L65 (2003).

[18] W. L. O'Brien and B. P. Tonner, Phys. Rev. B **49**, 15370 (1994).

[19] B. Schulz and K. Baberschke, Phys. Rev. B **50**, 13467 (1994).

[20] D. Sander, W. Pan, S. Ouazi, J. Kirschner, W. Meyer, M. Krause, S. Müller, L. Hammer, and K. Heinz, Phys. Rev. Lett. **93**, 247203 (2004).

[21] M. Y. Khan, C.-B. Wu, M. Erkovan, and W. Kuch, J. Appl. Phys. **113**, 023913 (2013).

[22] K. Sato, Jap. J. Appl. Phys. **20**, 2403 (1981).

[23] The slightly larger coercivity at 180 K can be attributed to the onset of exchange bias. Often a maximum of the coercivity as a function of temperature is observed close to the blocking temperature for exchange bias; see, for example, S. K. Mishra, F. Radu, H. A. Dürr, and W. Eberhardt, Phys. Rev. Lett. **102**, 177208 (2009); A. Behler, N. Teichert, B. Dutta, A. Waske, T. Hickel, A. Auge, A. Hütten, and J. Eckert, AIP Adv. **3**, 122112 (2013); or Ref. [26].

[24] K. Lenz, S. Zander, and W. Kuch, Phys. Rev. Lett. **98**, 237201 (2007).

[25] B. Zhang, C.-B. Wu, and W. Kuch, J. Appl. Phys. **115**, 233915 (2014).

[26] M. Y. Khan, C.-B. Wu, S. Kreft, and W. Kuch, J. Phys.: Condens. Matter **25**, 386005 (2013).

[27] S. Couet, K. Schlage, R. Rüffer, S. Stankov, T. Diederich, B. Laenens, and R. Röhlsberger, Phys. Rev. Lett. **103**, 097201 (2009).

[28] Hongtao Shi, D. Lederman, K. V. O'Donovan, and J. A. Borchers, Phys. Rev. B **69**, 214416 (2004).

[29] J. Zhu, Q. Li, J. X. Li, Z. Ding, J. H. Liang, X. Xiao, Y. M. Luo, C. Y. Hua, H.-J. Lin, T. W. Pi, Z. Hu, C. Won, and Y. Z. Wu, Phys. Rev. B **90**, 054403 (2014).

[30] E. E. Fullerton, K. T. Riggs, C. H. Sowers, S. D. Bader, and A. Berger, Phys. Rev. Lett. **75**, 330 (1995).

[31] M. Y. Khan, C.-B. Wu, and W. Kuch, Phys. Rev. B **89**, 094427 (2014).

[32] C. Won, Y. Z. Wu, H. W. Zhao, A. Scholl, A. Doran, W. Kim, T. L. Owens, X. F. Jin, and Z. Q. Qiu, Phys. Rev. B **71**, 024406 (2005).

[33] M. Ali, P. Adie, C. H. Marrows, D. Greig, B. J. Hickey, and R. L. Stamps, Nat. Mater. **6**, 70 (2007).

[34] W. Kuch, L. I. Chelaru, K. Fukumoto, F. Porrati, F. Offi, M. Kotsugi, and J. Kirschner, Phys. Rev. B **67**, 214403 (2003).

[35] P. J. Metaxas, R. L. Stamps, J.-P. Jamet, J. Ferré, V. Baltz, B. Rodmacq, and P. Politi, Phys. Rev. Lett. **104**, 237206 (2010).